Molecules and Cells

Increased Caveolin-2 Expression in Brain Endothelial Cells Promotes Age-Related Neuroinflammation

Hyunju Park[1,4], Jung A Shin[2,4], Jiwoo Lim[1], Seulgi Lee[1], Jung-Hyuck Ahn[3], Jihee Lee Kang[1], and Youn-Hee Choi[1,*]

[1]Department of Physiology, Inflammation-Cancer Microenvironment Research Center, Seoul 07804, Korea, [2]Department of Anatomy, Ewha Womans University College of Medicine, Seoul 07804, Korea, [3]Department of Biochemistry, Ewha Womans University College of Medicine, Seoul 07804, Korea, [4]These authors contributed equally to this work.
*Correspondence: yc@ewha.ac.kr
https://doi.org/10.14348/molcells.2022.0045
www.molcells.org

Aging is a major risk factor for common neurodegenerative diseases. Although multiple molecular, cellular, structural, and functional changes occur in the brain during aging, the involvement of caveolin-2 (Cav-2) in brain ageing remains unknown. We investigated Cav-2 expression in brains of aged mice and its effects on endothelial cells. The human umbilical vein endothelial cells (HUVECs) showed decreased THP-1 adhesion and infiltration when treated with Cav-2 siRNA compared to control siRNA. In contrast, Cav-2 overexpression increased THP-1 adhesion and infiltration in HUVECs. Increased expression of Cav-2 and iba-1 was observed in brains of old mice. Moreover, there were fewer iba-1–positive cells in the brains of aged Cav-2 knockout (KO) mice than of wild-type aged mice. The levels of several chemokines were higher in brains of aged wild-type mice than in young wild-type mice; moreover, chemokine levels were significantly lower in brains of young mice as well as aged Cav-2 KO mice than in their wild-type counterparts. Expression of PECAM1 and VE-cadherin proteins increased in brains of old wild-type mice but was barely detected in brains of young wild-type and Cav-2 KO mice. Collectively, our results suggest that Cav-2 expression increases in the endothelial cells of aged brain, and promotes leukocyte infiltration and age-associated neuroinflammation.

Keywords: aging, cav2$^{-/-}$ mouse, caveolin-2, endothelial cell, neuroinflammation

INTRODUCTION

Aging is characterized by a gradual functional decline (McHugh and Gil, 2018). In mammals, aging occurs heterogeneously across multiple organ systems, causing progressive deterioration that eventually results in tissue dysfunction (McHugh and Gil, 2018; Niccoli and Partridge, 2012). Many studies have shown that inflammation increases with advancing age, and most of the phenotypic characteristics observed in the aging process are the result of a low-grade chronic proinflammatory status called "inflammaging," which is characterized by increased production of proinflammatory cytokines, acute-phase proteins, reactive oxygen species (ROS), and autoantibodies (Finger et al., 2022; Melov, 2000; Snowdon et al., 2007). In the brain, aging causes changes in brain size, vasculature, and cognition and is considered a major risk factor for most common neurodegenerative diseases, including mild cognitive impairment, Alzheimer's disease, cerebrovascular disease, and Parkinson's disease (Hickman et al., 2018; Navarro et al., 2004; Williams and Lisanti, 2004).

Received 22 March, 2022; revised 30 August, 2022; accepted 12 October, 2022; published online 12 December, 2022

eISSN: 0219-1032

At the molecular level, mitochondrial function decreases owing to the accumulation of damaged mitochondria and ROS (Chakrabarti et al., 2011; Zia et al., 2021). Activated microglia exert beneficial functions, such as phagocytic clearance of pathogens and cellular debris. However, uncontrolled immune reactions induce neurological dysfunction (Flanary et al., 2007; Hefendehl et al., 2014). Age-related neuroinflammation results in an exaggerated production of proinflammatory cytokines, as well as other cytotoxic mediators, that can exert detrimental effects on neurons and contribute to cognitive dysfunction (Finger et al., 2022; Rea et al., 2018). During aging, microglia, as the primary mediators of the brain's immune responses, become dysregulated and contribute to a chronic state of neuroinflammation (Hickman et al., 2018). Although many studies have been conducted on changes in microglial phenotype and function and their effects on aging, little is known about the causal factors for age-associated microglial dysfunction, leukocyte recruitment, and initiation of the inflammatory microenvironment in the aging brain.

Caveolins, comprising caveolin-1 (Cav-1), Cav-2, and Cav-3, are a family of integral membrane proteins that are the principal components of caveolae membranes and are involved in receptor-independent endocytosis (Parat, 2009; Williams and Lisanti, 2004). They are involved in diverse cellular processes, ranging from cellular senescence, cell migration, cell cycle, and cell polarity, to regulate cell transformation and signal transduction by acting as scaffolding proteins within caveolar membranes by compartmentalizing and concentrating signaling molecules (Navarro et al., 2004; Parton and Simons, 2007; Williams and Lisanti, 2005; Zou et al., 2011). Moreover, caveolins participate in endocytosis and cholesterol transport (Krajewska and Maslowska, 2004; Le Lay et al., 2006; Parton and Simons, 2007). Cav-2 colocalizes with Cav-1 in caveolae, forms hetero-oligomers with Cav-1, is co-expressed in many of the same cells and tissues, and requires Cav-1 for proper membrane localization (Parolini et al., 1999; Scherer et al., 1997). Additionally, Cav-2 functions in various processes, such as angiogenesis, fibrosis, endocytosis, and regulation of inflammatory responses (de Almeida et al., 2011; Razani et al., 2002; Snowdon et al., 2007; Xie et al., 2010). Many studies have shown that Cav-1 is involved in cellular senescence or aging; however, the involvement of Cav-2 in this process is unknown. In this study, we investigated the expression of Cav-2 in the endothelial cells of the aged mouse brain. The results of this study will show the involvement of Cav-2 in age-related neuroinflammation.

MATERIALS AND METHODS

Reagents and antibodies

Antibodies against Cav-1 (Cat. No. 610406) and Cav-2 (Cat. No. 610685) were purchased from BD Biosciences (USA). Antibodies against actin and vascular endothelial (VE)-cadherin (Cat. No. sc9989) were purchased from Santa Cruz Biotechnology (USA). Antibodies against tubulin (Cat. No. T5168) and glial fibrillary acidic protein (GFAP; Cat. No. G 3893) were purchased from Sigma-Aldrich (USA). Antibodies against PECAM1 (Cat. No. ab28364) were purchased from Abcam (UK). Antibodies against iba-1 (Cat. No. 016-2000) were purchased from Wako (Japan).

Expression analysis in Gene Expression Omnibus (GEO) database

We selected gene expression datasets (GSE8150 [Reiter et al., 2007], GSE13120 [Oberdoerffer et al., 2008], GSE1572 [Lu et al., 2004], and GSE53890 [Lu et al., 2014]) from the GEO database. In GSE8150 and GSE13120, the neocortex tissues of 5- and 30-month-old mice were analyzed. In GSE1572 and GSE53890, the frontal cortex regions of young and old individuals were analyzed. The microarray datasets were normalized and applied to log2 transformation using R software.

Animals

All animals were housed and maintained in a pathogen-free environment/barrier facility at the Institute for Animal Studies at the Medical School of Ewha Womans University, and the experiments were performed in accordance with the international guidelines for the ethical use of experimental animals (IACUC No.17-0378). Cav-2 KO mice were purchased from the Laboratory Animal Resource Center (Korea Research Institute of Bioscience and Biotechnology, KRIBB). Wild-type C57BL/6N littermates were used as controls. B6C3F1 mice, obtained by crossing male C3H mice with female C57BL/6 mice which are used to genetic backgrounds on mouse models of neurodegenerative disorders such as Alzheimer's disease, were kindly gifted by Dr. Jung-Hyuck Ahn (Ewha Womans University, Seoul, Korea). In this study, mice aged 12-60 weeks were used.

Tissue preparation

Animals were deeply anesthetized by the intraperitoneal injection of zolazepam (12.5 mg/kg). The animals were initially perfused with phosphate-buffered saline (PBS) to rinse the blood. For molecular analysis, the brains were removed and stored at −80°C until use. For immunohistochemical analysis, the animals were perfused with 4% paraformaldehyde (PFA) in 0.01 M PBS for 5 min. After perfusion, the brains, livers, and kidneys were removed and fixed by immersion in 4% PFA solution overnight at 4°C. For immunohistochemical (IHC), tissues were embedded in paraffin and subsequently sectioned on a microtome at a thickness of 4 μm.

IHC and cell counts

Mouse tissues were processed for immunohistochemical analysis as described previously (Kim et al., 2011), with minor modification. Primary antibodies against Cav-1, Cav-2, PECAM1, VE-cadherin, GFAP, and iba-1 were used. All slides were counterstained with Mayer's hematoxylin, and negative controls were obtained by omitting primary antibodies from all slides. The numbers of iba-1 immunopositive cells under a 20× objective lens (area, 0.38 mm^2) for four randomly selected brain cortices were counted for each specimen, followed by the calculation of the mean number and SD. For double-labeling studies, the sections were incubated overnight in a mixture of the above-mentioned primary antibodies. To determine the expression level of each protein, digital images were obtained using a Zeiss LSM 710 (USA) confocal micro-

scope, and the brightness and contrast were adjusted using Adobe Photoshop 7.0 software (Adobe Systems, USA). All adjustments were performed equally across sections.

Pre-embedding IHC

Vibratome sections of 50 μm were processed for immunocytochemistry using an indirect pre-embedding immunoperoxidase method, as previously described (Han et al., 2004; 2005) with minor modifications. Briefly, the tissue sections were incubated with primary antibody against Cav-2 in a peroxidase-conjugated goat anti-mouse IgG Fab fragment (1:200; Jackson ImmunoResearch Laboratories, USA). For the detection of horseradish peroxidase (HRP), sections were incubated in a DAB+ Chromogen system (Dako, USA) for 5 min. Sections were postfixed with 2% glutaraldehyde and 2% PFA in 0.1 M phosphate buffer, followed by 2% osmium tetroxide. After rinsing, the sections were dehydrated and embedded in epoxy resin between polyethylene vinyl sheets. Appropriate areas of interest were selected from approximately 1 μm thick sections stained with toluidine blue. Approximately 60-70 nm ultrathin sections were cut by an ultramicrotome (Richer-Jung, USA) using a diamond knife. The thin sections were stained with 2% aqueous uranyl acetate and were imaged using an H-7650 transmission electron microscope (Hitachi, Japan) at an accelerating voltage of 80 kV.

Cell culture

Human umbilical vein endothelial cells (HUVECs) were obtained from Dr. Kihwan Kwon (Ewha Womans University, Seoul, Korea) and cultured as described previously (Jeon et al., 2015). HUVECs at passage 8 were used in this study and maintained in Medium 200 (Life Technologies, USA) with 5% fetal bovine serum (FBS; Gibco, USA), 1% penicillin-streptomycin, and low-serum growth supplement (Life Technologies) in a humidified incubator containing 5% CO_2 at 37°C. THP-1 human acute monocytic leukemia cells were obtained from the American Type Culture Collection (USA) and grown in RPMI 1640 medium (WelGENE, Korea) supplemented with 10% FBS and 1% penicillin-streptomycin and maintained at 37°C in a humidified atmosphere of 5% CO_2 and 95% air.

siRNA transfection

The HUVECs were transiently transfected with SMART pools human Cav-2 siRNA (Dharmacon, USA) using Lipofectamine® reagent (Invitrogen, USA) according to the manufacturer's instructions (Jeon et al., 2015). Green fluorescence protein (GFP) siRNA (Bioneer, Korea) was used as a control. After 48 h of transfection, the cells were used for subsequent experiments.

Lentivirus-mediated Cav-2 overexpression

To obtain stable Cav-2-overexpressing HUVECs, pLenti-GIII-CMV-GFP-2A-Puro vector (Abcam) was transfected into 293T cells along with the packaging plasmids (psPAX2 and pCMV VSV G) using Metafectene PRO (Biontex, Germany). Lentiviral particles containing media were collected and filtered 48 h after transfection. The HUVECs were infected by replacing the medium lentivirus particles with polybrene (final concentration of 8 μg/ml). The medium was removed and replaced with a fresh medium after 24 h of incubation. The HUVECs were incubated in a medium containing puromycin (3 μg/ml) to select for stable cell lines. Lentiviral-based Cav-2 overexpression was performed by western blotting.

Western blot analysis

For the preparation of brain lysates, fresh whole mouse brain tissues were lysed using a sonicator (Bioruptor® Plus sonication device; Diagenode, UK) in 200 μl of ice-cold radioimmunoprecipitation assay (RIPA) lysis buffer (Park et al., 2017) with Xpert protease inhibitor cocktail (GenDEPOT, USA). Total proteins were resolved on 12% sodium dodecyl sulfate-polyacrylamide gels and transferred onto polyvinylidene fluoride membranes (Amersham Pharmacia Biotech, Sweden). The membranes were blocked with 5% skim milk for 1 h at room temperature and then incubated at 4°C overnight with primary antibodies and HRP-conjugated secondary antibodies (Santa Cruz Biotechnology). Protein bands were visualized using the chemiluminescence method (GE Healthcare, UK).

Endocytosis assay

HUVECs (control [Cont], Lenti-Cav-2, GFP siRNA, and Cav-2 siRNA) were incubated for 5, 15, and 30 min in 50 nM BOIPY® FL C5-lactosylceramide (Invitrogen). For microscopic analysis, cells were washed three times in PBS and fixed in 4% PFA for 10 min at room temperature. The fixed cells were washed twice with PBS. The preparations were then mounted and observed using a confocal microscope (LSM800; Zeiss, Germany). Quantification was performed using ImageJ software (National Institutes of Health [NIH], USA; http://rsb.info.nih.gov/ij/).

Adhesion assay

THP-1 cells were fluorescently labeled with 5 μM calcein AM (BCECF/AM; Invitrogen) for 30 min at 37°C in RPMI 1640 medium containing 10% FBS. HUVECs (Cont, Lenti-Cav-2, GFP siRNA, and Cav-2 siRNA) were seeded in 96-well plates at a density of 1×10^4 cells/ml in a 5% CO_2 incubator. THP-1 cells were washed twice with the medium, after which calcein AM-labeled THP-1 cells (3×10^5 cells) in 0.1 ml of the medium were added to each HUVEC-containing well and incubated for 2 h. The non-adherent THP-1 cells were removed by gentle washing twice with PBS. Adherent monocytes were observed using a fluorescence microscope (Axiovert 200; Zeiss).

Endothelial transmigration assay

Transmigration was examined using 3-μm pore Transwell chambers (Corning, USA) coated with gelatin according to the manufacturer's instructions (Guo et al., 2021). HUVECs (Cont, Lenti-Cav-2, GFP siRNA, and Cav-2 siRNA) were seeded into the upper chambers at 2×10^5 cells/well for 24 h, and THP-1 cells were then added to the upper chamber of Transwells containing the endothelial cell monolayer in serum-free RPMI 1640 medium. RPMI 1640 medium supplemented with 10% FBS was added to the bottom wells. Transmigrated monocytes were identified after 24, 48, and 72 h by counting cells in the lower chamber.

Primary cortical endothelial and microglia separation

The mechanical dissociation of the brain cortex tissue was performed using the Adult Brain Dissociation Kit (Miltenyi Biotec, Germany) and Gentle MACS dissociator (Miltenyi Biotec) according to the manufacturer's protocols. Endothelial and microglial cells were separated from the remaining cells using magnetic cell sorting. For endothelial cell separation, the cells from the whole brain cortex (n = 4, each group) were resuspended with CD45 microbeads (Miltenyi Biotec) and passed through an MS column. The flow-through containing CD45-negative unlabeled cells was collected and centrifuged (300 × *g*, 10 min). After removal of the supernatant, the cells were incubated with CD31 microbeads (Miltenyi Biotec) and then passed through an MS column. The CD31-positive cells that remained in the column were washed out and collected by firmly pushing the plunger into the column. CD45-negative cells and CD31-positive cells were isolated using the above procedure. For microglial cell separation, the cells were resuspended with CD11 microbeads (Miltenyi Biotec), and then the CD11-positive cells that remained in the MS column were washed out and collected by firmly pushing the plunger into the column. Microglial cells were counted using a hemocytometer.

Proteome profiler mouse XL cytokine array

The cortex tissue lysates from wild-type mice (3 and 15 months old) and Cav-2 KO mice (3 and 15 months old) were measured using a Mouse XL Cytokine Array Kit (Cat. No.

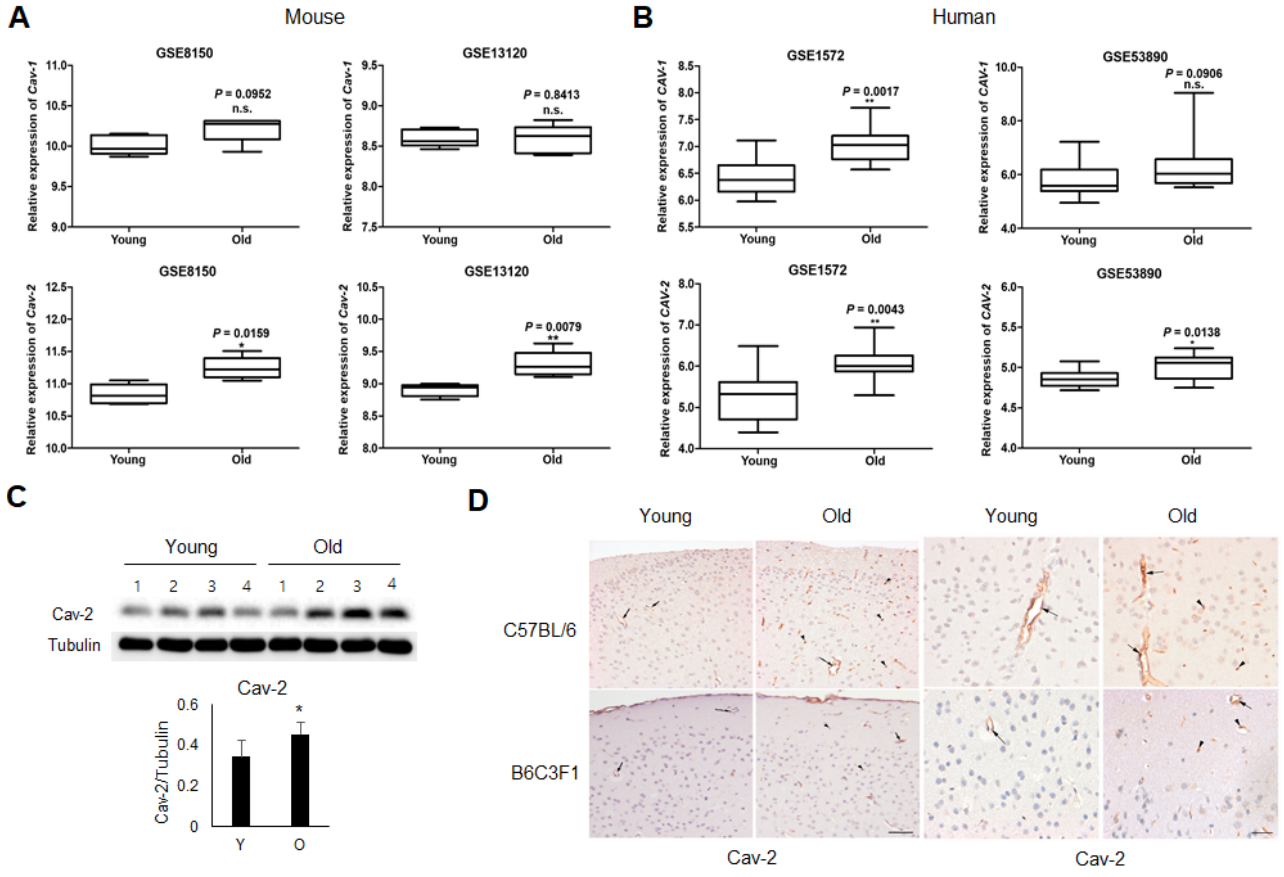

Fig. 1. Caveolin-2 (Cav-2) expression is increased in the aged mice brain. (A) Relative *Cav-1* and *Cav-2* mRNA expression levels were compared in the neocortex tissues of young (5 months old) and old (30 months old) mice samples from microarray datasets in the Gene Expression Omnibus (GEO) database (GSE8150 and GSE13120). Unpaired, non-parametric Mann-Whitney U test was used to compare the difference in *Cav-1* and *Cav-2* expression between the young and old mice groups in GEO datasets. n.s., not significant. $*P < 0.05$, $**P < 0.01$ between young and old mice groups. (B) Relative *CAV-1* and *CAV-2* mRNA expression levels were compared in the neocortex of young and old individuals from microarray datasets in the GEO database (GSE1572 and GSE53890). Unpaired, non-parametric Mann-Whitney U test was used to compare the difference in *CAV-1* and *CAV-2* mRNA expression between the young and old human groups in GEO datasets. n.s., not significant. $*P < 0.05$, $**P < 0.01$ between young and old human groups. (C) Fifteen micrograms of whole-cell lysates from the cerebral cortex of 3-month-old (young, Y) and 15-month-old (old, O) mice were analyzed by immunoblotting against total Cav-2. Tubulin was used as the loading control. The graph represents the normalized intensities of caveolins against those of tubulin determined from three independent experiments (n = 4). The bars represent SD. $*P < 0.05$. (D) Immunohistochemical staining for Cav-2 protein was performed for the cerebral cortex of 3-month-old (young) and 15-month-old (old) C57BL/6 and B6C3F1 mice. Scale bars = 20 μm in left and 50 μm in right. Representative images show immunoreactivity of Cav-2 (arrows and arrowheads).

ARY028; R&D Systems, USA) according to the manufacturer's instructions. Briefly, membranes were blocked with blocking buffer for 1 h, incubated with each sample (200 μg) overnight at 4°C, and pre-incubated for 1 h with a biotinylated detection antibody cocktail. Membranes were then incubated with streptavidin-HRP for 30 min and washed with wash buffer. The levels of cytokines/chemokines were measured by the spot intensity using ImageJ software and visualized using Morpheus (https://software.broadinstitute.org/morpheus).

Serum protein concentrations

Whole blood was collected from the mouse vein. Serum samples were obtained by centrifuging the blood samples at 3,000 rpm for 10 min. The levels of CRP, MCP-2, MMP-2, and MMP-3 in diluted serum were analyzed in Komabiotech via Magnetic Luminex® Screening Assay (R&D Systems) according to the manufacturer's protocol.

Statistical analysis

Statistical analyses were performed using Student's *t*-test to compare differences between the sample groups, and ANOVA was used to determine differences among multiple groups. Statistical significance was set at $P < 0.05$. In GEO dataset analysis, unpaired, non-parametric Mann–Whitney U test was performed using Prism 5.0 software (GraphPad Software, USA).

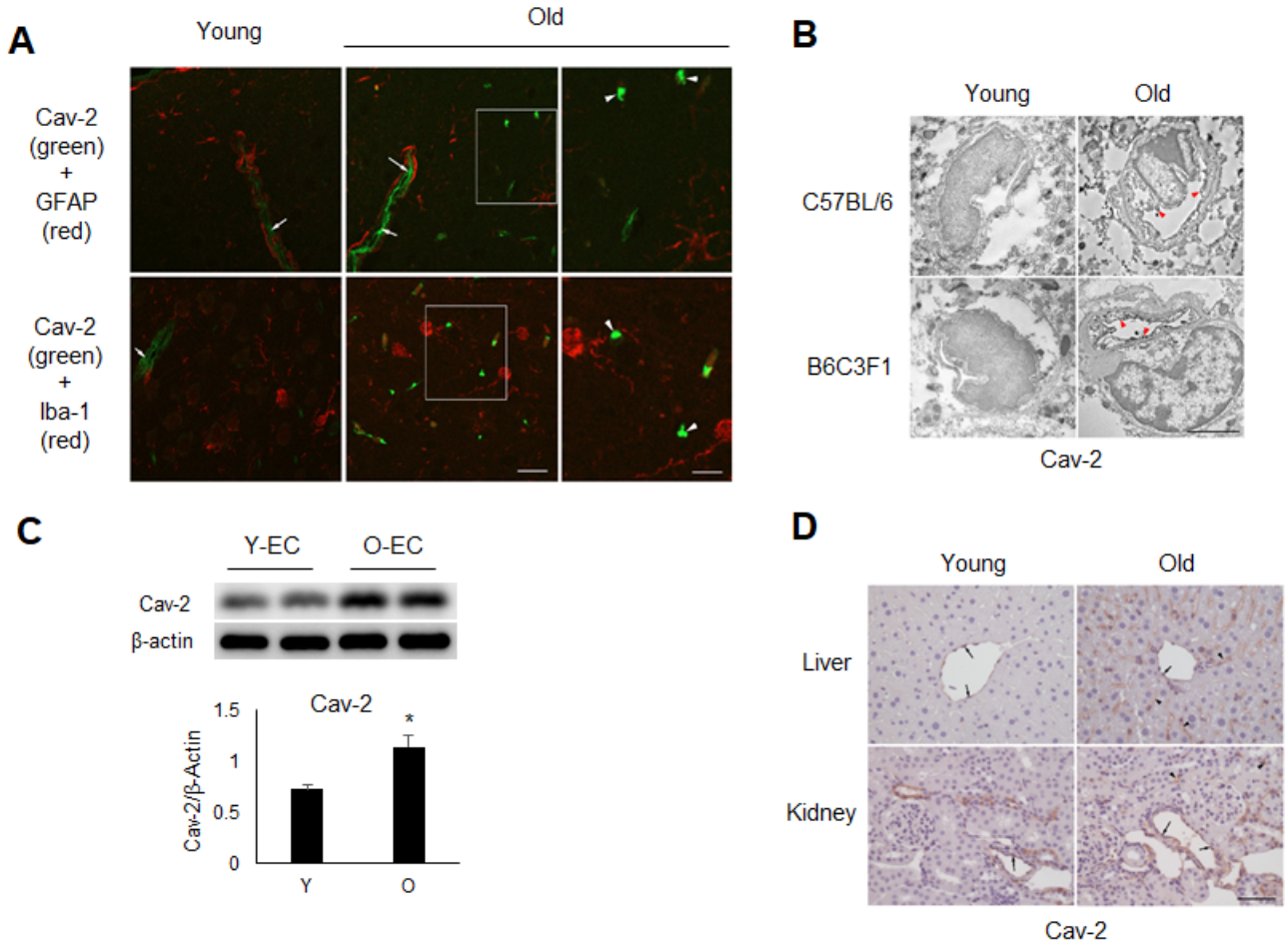

Fig. 2. Cav-2 expression increases in the endothelial cells of aged brain. (A) Immunohistochemical staining revealed that caveolin-2 (Cav-2) (green) expression is increased in endothelial cells (arrows and arrowheads) of aged mouse brain, but not astrocytes (GFAP, red) or microglia (iba-1, red). Scale bars = 20 μm in middle panel and 10 μm in right panel. (B) Pre-embedding immunohistochemistry for Cav-2 in the cortex of 3-month-old and 15-month-old C57BL/6 and B6C3F1 mice showed immunostaining at the apical side of endothelial cells (arrowheads) in old mice. Scale bar = 5 μm. (C) Primary cortical endothelial cells were separated using the Endothelial Cell Isolation Kit (Miltenyi Biotec, Germany). Eight micrograms of cell lysates in cold-RIPA buffer was extracted and analyzed by immunoblotting against Cav-2. The graph represents the normalized intensities of Cav-2 against those of β-actin determined from three independent experiments (n = 6). The bars represent SD. Y-EC, young-endothelial cell; O-EC, old-endothelial cell. $*P < 0.05$. (D) Immunohistochemical staining for Cav-2 protein was performed using the liver and kidney of 3-month-old (young) and 15-month-old (old) C57BL/6 mice. Scale bar = 50 μm. Immunostaining in both large (arrows) and small (arrowheads) vessels were observed in the liver and kidney of old mice, while immunostaining in large vessels (arrows) were observed in young tissues. Data shown are representative of at least three experiments.

RESULTS

Cav-2 expression is increased in aged mouse brain

A previous study demonstrated that the extent of mRNA expression is largely affected by the aging process (Lu et al., 2004). To explore the effect of normal aging on *Cav* gene expression, we selected gene expression datasets of mice and humans from the GEO database. In two independent mouse datasets, *Cav-2* mRNA was overexpressed in old mouse brain samples compared with young mice samples (Fig. 1A, young and old mice in GSE8150 and GSE13120). Similar to mouse data, in two independent human datasets, *Cav-2* mRNA was consistently increased in aged groups compared with younger groups (Fig. 1B, young and old individuals in GSE1572 and GSE53890). *Cav-2* mRNA expression was significantly increased in GSE8150, GSE13120, GSE1572, and GSE53890 in old brain samples compared with young samples, whereas an increase in *Cav-1* mRNA expression in the aged brain samples compared with the young samples was observed in only one human dataset GSE1572, but not in mouse data. To test whether Cav-2 protein expression is increased in aged mice, we analyzed whole-cell lysates obtained from the cerebral cortex of 3-month-old (young) and 15-month-old (old) C57BL/6 mice by immunoblotting against Cav-2. Cav-2 expression was significantly increased in old mice (Fig. 1C). To determine whether Cav-2 expression is increased in aged mice with different mouse strains, we performed a similar experiment in B6C3F1. Cortex tissues from two different types of mice, C57BL/6 and B6C3F1, were immunohistochemically stained for Cav-2, and an increase in Cav-2 expression was observed in old mice, especially in small and large vessels (Fig. 1D).

Cav-2 expression is increased in endothelial cells of aged mouse brain, but not astrocytes or microglia

To determine whether Cav-2 expression is increased in different types of brain cells, we performed immunofluorescence assays using cortex tissues. A merged immunofluorescence image of astrocytes stained with GFAP or microglia stained with iba-1 revealed rarely colocalization with staining of Cav-2 (Fig. 2A). To confirm that the cell type expressed increased Cav-2 in old mouse brains, pre-embedding immunofluorescence was employed by transmission electron microscopy (TEM) (Fig. 2B). TEM images showed that Cav-2 was expressed specifically in VE cells in old mice. We next determined the isolation of primary cortical endothelial cells

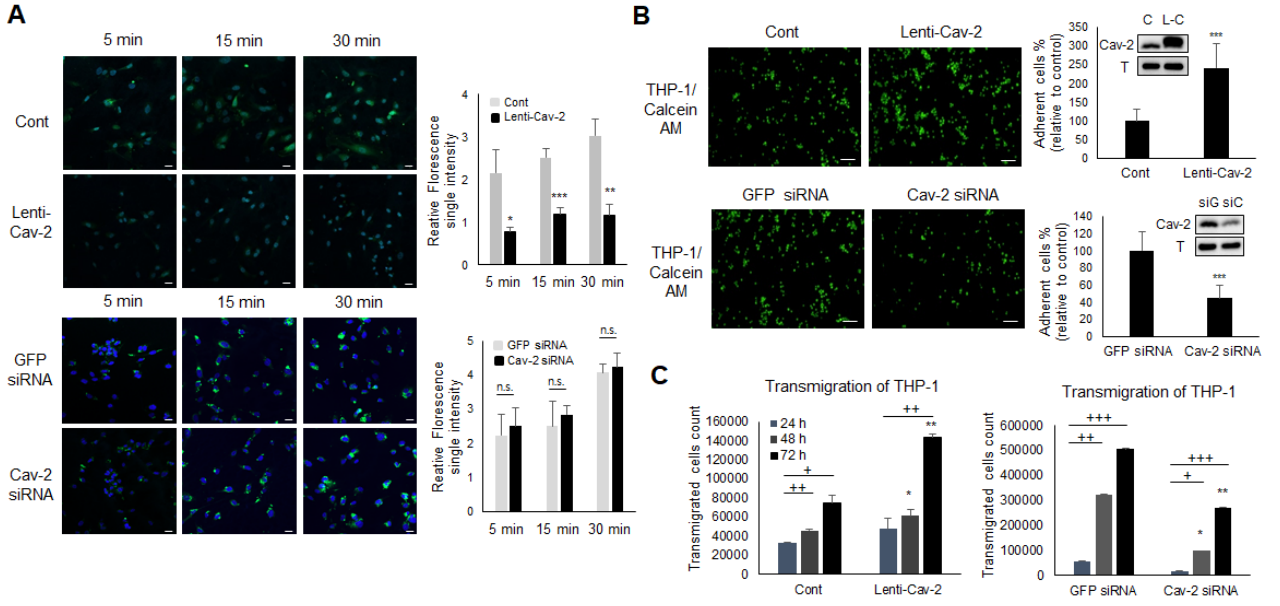

Fig. 3. Cav-2 induces adhesion and transmigration of THP-1 cells. (A) The lenti- control (Cont) human umbilical vein endothelial cells (HUVECs), lenti-Cav-2 HUVECs, and HUVECs transfected with siRNA for GFP or Cav-2 for 48 h were incubated with 50 nM BOIPY® FL C5-lactosylceramide-conjugated transferrin for the indicated times. The cells were then fixed and observed by confocal microscopy. The mean value of the intensity of each experiment was acquired by measuring the intensity of at least three random fields. Scale bars = 20 μm. n.s., not significant. (B) Functional role of Cav-2 on monocyte adhesion to endothelial cells. The lenti-Ctrl HUVECs (Cont), lenti-Cav-2 HUVECs, and HUVECs transfected with siRNA for GFP or Cav-2 for 48 h, were co-cultured with calcein AM-labeled THP-1 monocytes for 1 h. Green spots represent calcein AM-labeled adherent THP-1 cells. Microphotographs (three independent experiments) were obtained using a fluorescence microscope. Scale bars = 100 μm. T, tubulin. (C) The lenti-Ctrl HUVECs (Cont), lenti-Cav-2 HUVECs, and HUVECs transfected with siRNA for GFP or Cav-2 for 48 h were cultured in Transwell chambers coated with 0.1% gelatin on its lower surface. Subsequently, THP-1 cells were added to the wells and incubated for 24, 48, and 72 h. THP-1 cells migrated to the lower compartment of the Transwell chambers. The THP-1 cell migration ability was defined by the number of THP-1 cells migrated. The experiments were performed in triplicate. The bars represent SD. $*P < 0.05$, $**P < 0.01$, $***P < 0.001$ compared with control HUVECs. $^{+}P < 0.05$, $^{++}P < 0.01$, $^{+++}P < 0.001$ as indicated.

by MACS immunomagnetic cell separation from young and old mice and performed immunoblotting against Cav-2 with the enrichment of purified endothelial cells. We observed increased Cav-2 expression in purified endothelial cells of old mouse brains compared with those of young mouse brains (Fig. 2C). To test the increased expression of Cav-2 protein in other organs, the liver and kidney were analyzed by immunohistochemistry using a Cav-2 antibody. Immunopositive Cav-2 protein was detected in both large and small blood vessels in the old liver and kidney, whereas only large vessels were stained in the young tissues (Fig. 2D).

Cav-2 induces adhesion and transmigration of THP-1 cells

To test whether increased expression of Cav-2 is involved in endocytosis, we performed an endocytosis assay using fluorescent C5-lactosylceramide. Cav-2-overexpressing HUVECs showed decreased C5-lactosylceramide internalization/endocytosis activity, whereas Cav-2 knockdown HUVECs did not show significant differences in endocytosis activity compared with control cells (Fig. 3A). As a result of RNA-seq analysis of genes affected by the increase in caveolin expression using stable Cav-2-overexpressing HUVECs, we found that the increase or decrease of genes affecting cell adhesion were observed when caveolin expression was increased (Supplementary Materials and Methods, Supplementary Fig. S1). To test whether the increased expression of Cav-2 affects adhesion and transmigration of monocytes, we performed adhesion and endothelial transmigration assays using a fluorescently

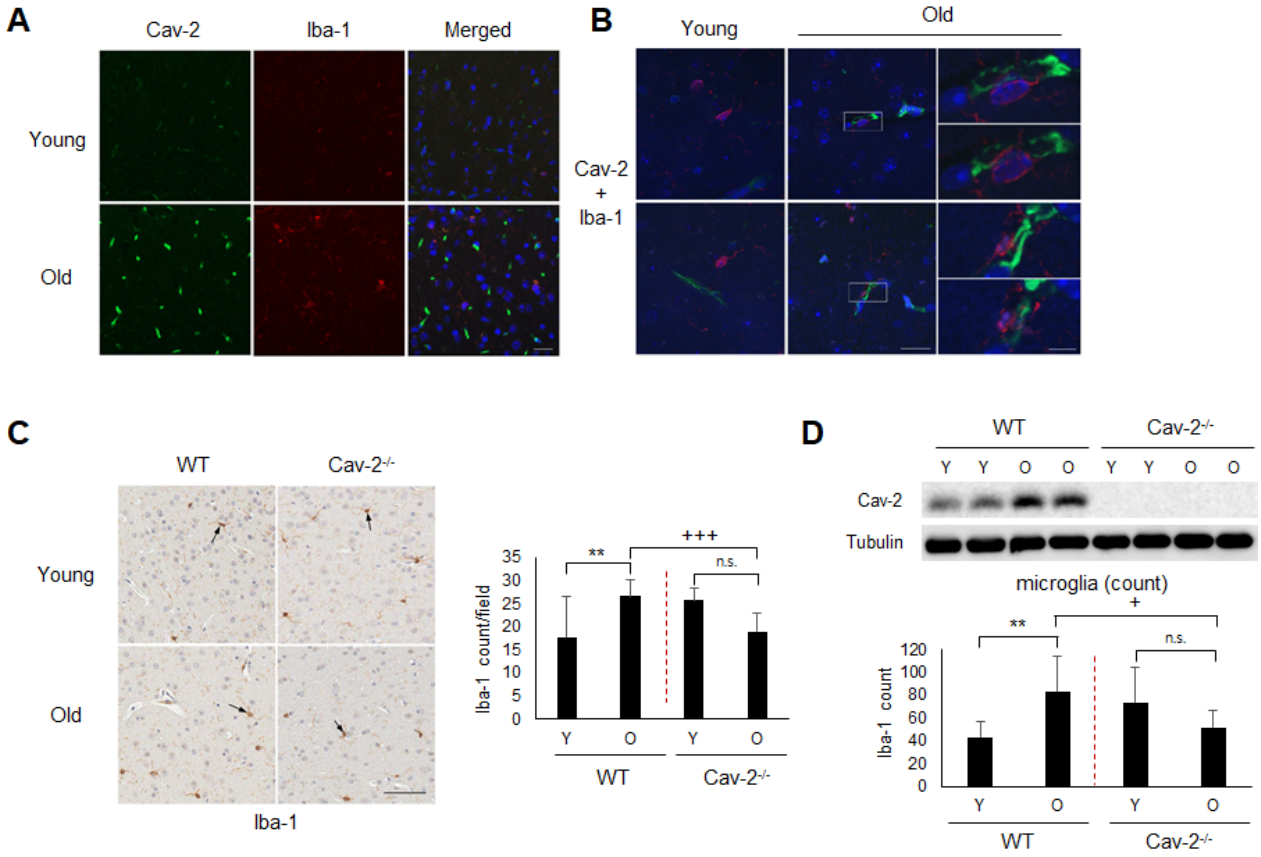

Fig. 4. Cav-2 affects leukocyte infiltration in the brain tissue. (A) Double staining for Cav-2 and iba-1 protein in the cerebral cortex of 3 month old (young) and 15-month-old (old) C57BL/6 mice. Tissues were immunostained with primary antibodies against Cav-2 and the microglia marker iba-1. Nuclei were stained with DAPI. The experiment was repeated at least three times, with similar results. Scale bar = 20 μm. (B) Boxed areas of Cav-2-positive microvessels in the cerebral cortex of old mice are shown as a Z-stack projection image (right panel). iba-1-positive microglia infiltrate through Cav-2-positive endothelial cells in old mice. Scale bars = 10 μm. (C) Immunohistochemical staining for iba-1 protein in the cerebral cortex of young (Y; 3 months old) or old (O; 15 months old) wild-type (WT) and Cav-2 knockout (KO) mice. Number of iba-1 immunopositive cells (arrows) were counted in 0.38 mm^2 area in the cerebral cortex of young or old wild-type and Cav-2 KO mice. Scale bar = 60 μm. n.s., not significant. (D) Examination of Cav-2 protein expression levels in the cerebral cortex of 3-month-old (young) and 15-month-old (old) mice wild-type and Cav-2 KO mice by western blot. Primary mouse cortical microglia cells were isolated using CD11b (Miltenyi Biotec) microbeads and CD11b/c (Miltenyi Biotec) microbeads. Microglia cells were counted using a hemocytometer in the cerebral cortex of young (3 months old) or old (15 months old) wild-type and Cav-2 KO mice. Data are representative of the results of three separate experiments. The bars represent SD. $^{**}P < 0.01$ versus young wild-type. $^{+}P < 0.05$, $^{+++}P < 0.001$ versus old wild-type.

labeled THP-1 monocyte cell line. Cav-2-overexpressing HUVECs showed a significant increase in THP-1 adhesion and endothelial transmigration, whereas Cav-2 small interfering RNA (siRNA)-treated HUVECs showed a significant decrease in THP-1 adhesion and endothelial transmigration compared with control GFP siRNA-treated cells (Figs. 3B and 3C).

Cav-2 induces leukocyte infiltration in brain tissue

When cortex tissues were analyzed by immunofluorescence staining for Cav-2 and iba-1, we observed increased Cav-2 and iba-1 expression in old mice (Fig. 4A). Although the expression levels of these two proteins were increased in old mice, a merged immunofluorescence image of Cav-2 or iba-1 revealed barely detectable colocalization as assessed by the occurrence of yellow fluorescence. However, an enlarged image showed that iba-1–positive cells were localized close to Cav-2-positive endothelial cells and, in some areas, iba-1–positive microglia passed through endothelial cells (Fig. 4B). To examine an increase in the levels of protein or an increase in cell number, histological quantification of brain tissue for iba-1–positive cells was performed using Cav-2 KO mice (Fig. 4C). In wild-type mice, the number of iba-1–positive cells was increased in the old mouse brain compared with the young mouse brain. In contrast, in Cav-2 KO mice, an increase in cell count was observed in young mice, and a significant decrease in cell count was found in old mice. To test whether the number of microglia is increased in the old mouse brain, primary cortical microglia separation was performed by isolating microglia from a mouse brain kit. Aged wild-type mouse brains showed increased microglia numbers compared with young wild-type mouse brains, whereas aged Cav-2 KO mouse brains did not show a significant difference in microglia number compared with young Cav-2 KO mouse brains (Fig. 4D).

Cav-2 deficiency reduces the level of chemokine expression in brain tissue

To investigate whether aging or Cav-2 deficiency affects chemokine expression, a chemokine array was performed using young and aged wild-type and Cav-2-deficient mice. We found that 47 chemokines, including CXCL10, ANGPT-L3, CXCL11, and CCL11 (out of 111 chemokines tested), were highly expressed in aged wild-type mice compared with other groups (Fig. 5A). Further, 36 chemokines were upregulated more than two-fold in aged wild-type mice than in young wild-type mice, whereas 59 chemokines showed over two-fold increase in aged wild-type mice compare with their expression in aged Cav-2 KO mice (Supplementary Fig. S2). Since the increase in chemokine expression indicated brain inflammation in aged wild-type mice, we next analyzed serum protein levels to determine whether systemic inflammation was also present in aged mice. The total blood levels of C-reactive protein (CRP), monocyte chemotactic protein-2 (MCP-2), matrix metalloproteinase-2 (MMP-2), and matrix metalloproteinase-3 (MMP-3), which are commonly used to detect systemic inflammation due to acute conditions or monitor the severity of disease in chronic conditions of inflammation in the blood, were not significantly changed, or even decreased, both in aged wild-type and Cav-2 KO mice (Fig. 5B).

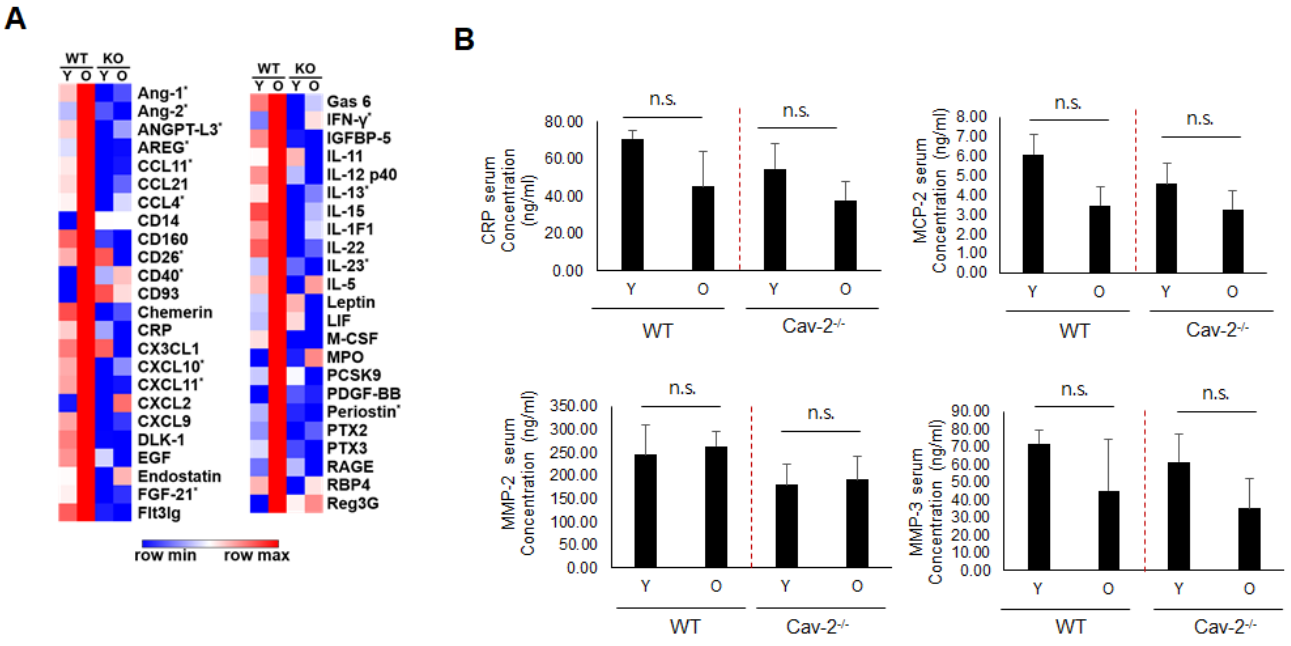

Fig. 5. Cav-2 affects the level of cytokine expression in the brain tissue. (A) Two hundred micrograms of whole-cell lysates from the cerebral cortex of young (Y; 3 months old) and old (O; 15 months old) wild-type (WT) and Cav-2 knockout (KO) mice were analyzed by the cytokine array kit as described in Materials and Methods section. The heatmap shows the expression levels of the cytokines. (B) Determination of the serum concentration of the C-reactive protein (CRP), monocyte chemotactic protein-2 (MCP-2), matrix metalloproteinase-2 (MMP-2), and matrix metalloproteinase-3 (MMP-3) ratio in young (3 months old) or old (15 months old) wild-type (WT) and Cav-2 KO mice. n = 5 to 8 per group. n.s., not significant.

Expression of PECAM1 and VE-cadherin is increased in aging brain in Cav-2-dependent manner

To explore the effect of aging on the expression levels of adhesion molecules, we analyzed gene expression datasets of mice and humans from the GEO database (Fig. 1). In independent mouse and human datasets, the expression of *PECAM1* and *VE-cadherin* mRNA was found to be increased in the brains of aged group compared with that in the young group (Fig. 6A, young and old mice in GSE13120 and humans in GSE53890). Next, in order to confirm whether there is an increase in PECAM1 and VE-cadherin protein expression in our animal model, we performed IHC on cortical tissues from young and old mice. The expression of PECAM1 and VE-cadherin proteins was increased in the brains of aged wild-type mice, but it was barely detected in those of young mice (Fig. 6B). In Cav-2 KO mice, PECAM1 and VE-cadherin protein expression was reduced or abolished even in the brains of old mice (Fig. 6C).

DISCUSSION

In this study, we demonstrated for the first time that Cav-2 expression was increased in the endothelial cells of the aging brain and that the increase in Cav-2 enhanced the adhesion

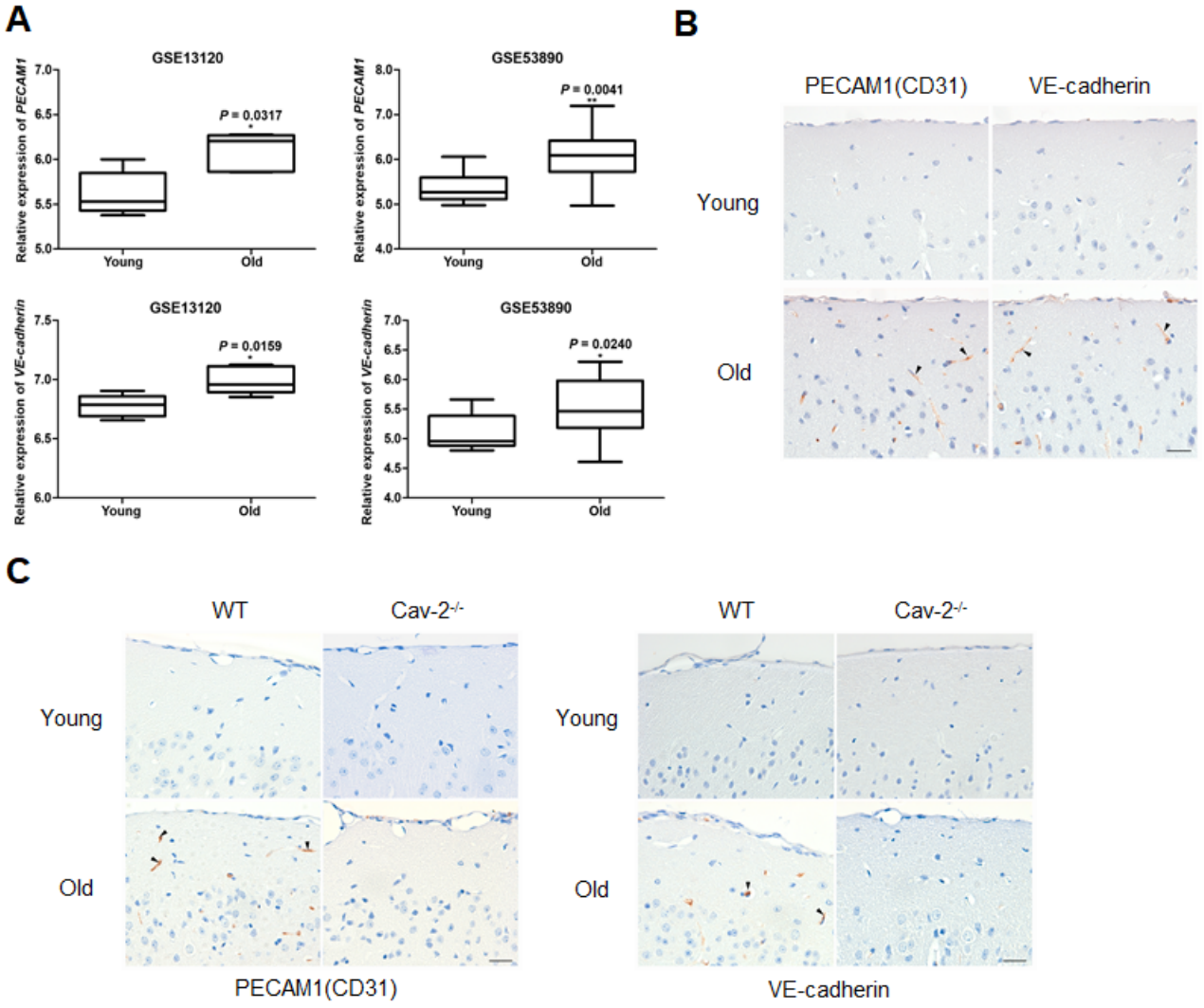

Fig. 6. The expression of PECAM1 and VE-cadherin is increased in the aging brain in a Cav-2-dependent manner. (A) Left, relative *PECAM1* and *VE-cadherin* mRNA expression levels were compared in the neocortex tissues of young (5 months old) and old (30 months old) mice from a microarray dataset in the Gene Expression Omnibus (GEO) database (GSE13120). Right, relative *PECAM1* and *VE-cadherin* mRNA expression levels were compared in the neocortex of young and old mice from a microarray dataset in the GEO database (GSE53890). Unpaired, non-parametric Mann-Whitney U test was used to compare the gene expression difference between young and old groups in each GEO dataset. $*P < 0.05$, $**P < 0.01$ between the young and old groups. (B) Immunohistochemical staining for PECAM1 and VE-cadherin protein was performed using the cerebral cortex of 3-month-old (young) and 15-month-old (old) C57BL/6 mice (scale bar = 50 μm) and (C) Cav-2 knockout (KO) mice (scale bars = 50 μm). Representative images show the immunoreactivity of PECAM1 and VE-cadherin (left, arrowheads). WT, wild-type.

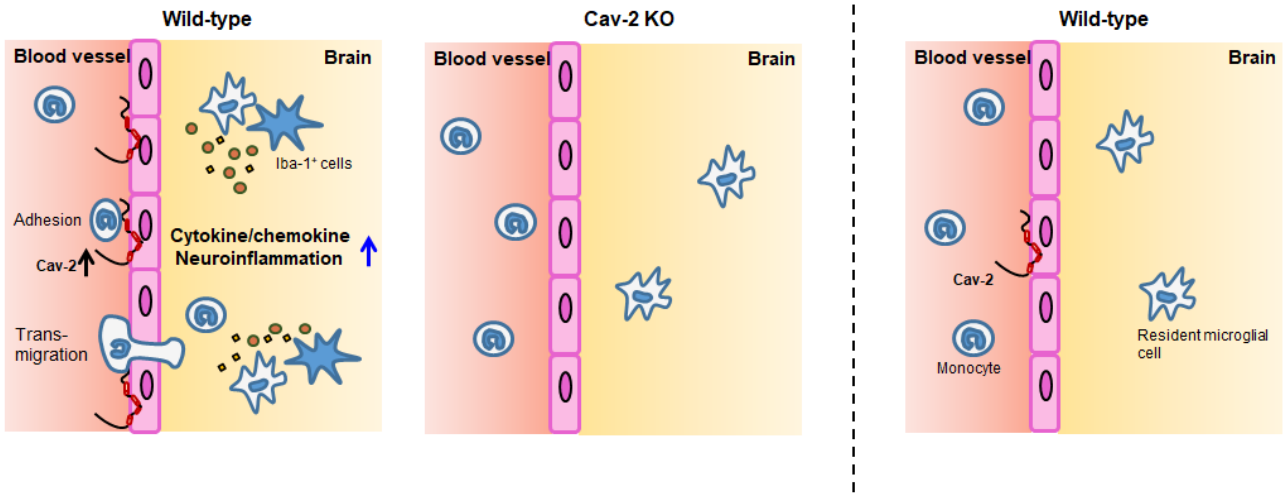

Fig. 7. Schematic model depicting the Cav-2 in age-related neuroinflammation. Cav-2 expression is increased in the endothelial cells of the aging brain, and the increased Cav-2 level enhances the adhesion and transendothelial migration of leukocytes. Compared with aged wild-type mice, aged Cav-2 knockout (KO) mice showed decreased number of iba-1 positive cells and reduced chemokine expression in brain tissues, suggesting the increase in Cav-2 level plays a key role in the age-related neuroinflammation.

and transendothelial migration of leukocytes. Interestingly, the number of iba-1–positive cells and the expression level of chemokines were significantly lower in aged Cav-2 KO mice than in age-matched wild-type mice, suggesting a role of Cav-2 in the establishment of the age-mediated inflammatory environment in the brain. Recent insights into age-related neuroinflammation have shown an exaggerated production of proinflammatory cytokines and other cytotoxic mediators, such as ROS, and infiltration of blood-borne immune cells that can exert detrimental effects on neurons and contribute to cognitive dysfunction and neuroinflammation (Sevenich, 2018). Our results provide initial evidence that increased expression of Cav-2 in brain endothelial cells is involved in age-related neuroinflammation.

In our study, Cav-2 in endothelial cells of aged mice seems to be responsible for novel inflammatory functions. Cav-1 has been well-documented to play an important role in cell adhesion (Duxbury et al., 2004; Wei et al., 1999; Xu et al., 2013), and our results showed that both knockdown and overexpression of Cav-2 alone significantly affected the adhesion and transmigration of THP-1 cells, suggesting a role of endothelial Cav-2 in regulating leukocyte adhesion and transmigration. In endocytosis experiments, the overexpression of Cav-2 reduced the internalization of C5-lactosylceramide, but Cav-2 knockdown did not affect this event in HUVECs. Similar to our results, a previous report showed that Cav-2 expression inhibited receptor endocytosis of the plasma membrane of the M1 muscarinic acetylcholine receptor and oligomerization of Cav-1 (Shmuel et al., 2007). Several reports have revealed the distinct activity of Cav-1 and Cav-2, suggesting that these proteins act antagonistically or independently in the regulation of some cellular processes (de Almeida et al., 2011; Shmuel et al., 2007; Zhan et al., 2017). Our results obtained from Cav-2 KO mice strongly suggest that Cav-2 performs a different function in the aging process than Cav-1, which is beyond the known functions that work with Cav-1. Therefore, research in aging with studies involving Cav-2 should be conducted in the future to reveal the pathophysiological significance of Cav-2.

Chemokine array data obtained from young and old wild-type mice showed that an aging brain is accompanied by inflammation. Although an increase in 85% of the chemokines tested (94 out of 111 chemokines) was observed in old wild-type mice (Supplementary Fig. S2), given that the chemokine expression levels in the tissue were not high and no increase in blood CRP, MCP-2, MMP-2, and MMP-3 levels was observed (Fig. 5), a low-grade inflammatory response may have occurred in the brain tissue during aging. Many studies have been performed to explain how inflammation leads to accelerated brain aging and neurodegenerative diseases, but not much has been done on the effect of aging on the molecular mechanisms of brain inflammation. In this study, we focused on analyzing the differences between older wild-type and older Cav-2 KO mice and found that Cav-2 deficiency significantly decreased chemokine expression and the number of infiltrating iba-1–positive cells in older mice, indicating a potential direct causal role of Cav-2 in age-related neuroinflammation. Interestingly, we noticed that the number of infiltrating iba-1–positive cells was higher in 3-month-old Cav-2 KO mice than in 3-month-old wild-type mice. Moreover, we found that the expression levels of 10 chemokines were higher in young Cav-2 KO mice than in the other three groups (Supplementary Fig. S2). These results suggest that the changes that occur in brain tissues vary by age group during aging in Cav-2-deficient mice. Cav-2 deficiency seems to induce the expression of several chemokines in young mice, which is largely different from that in older mice; therefore, we hypothesize the phenomena induced by Cav-2 deficiency in young mice but have not yet explained the mechanism due to loss of function or compensation and are currently trying to understand this phenomenon using RNA-seq analysis by age group between wild-type and Cav-2 KO mice.

In our study, the expression of Cav-1 remained unchanged in both HUVEC cell lines and mouse models with altered Cav-2 expression (Supplementary Fig. S3). We found an increase in Cav-1 only in aged wild-type mice by IHC and immunoblotting. In IHC, we found that the expression of Cav-1, as well as Cav-2, was increased in the aged brain compared with the young brain (Supplementary Fig. S4). Cav-2 is known to maintain protein stability only when Cav-1 is present. In the absence of Cav-1, Cav-2 is degraded, and its expression is markedly reduced (Drab et al., 2001; Razani et al., 2001; Sowa, 2011). Although we did not examine the involvement of Cav-1 in this study, considering the results from previous studies, the persistence of Cav-1 expression, which is expressed more than a certain amount, may help stabilize the function of Cav-2 protein. There are many reports on the role of Cav-1 in the aging process (Park et al., 2000; Volonte and Galbiati, 2020; Volonte et al., 2002; Wheaton et al., 2001); however, this is the first study to report the role of Cav-2 in age-related neuroinflammation. We have previously reported the differential expression of Cav-1 in astrocytes and microglia, wherein it provided neuroprotection against exogenous ROS, especially in astrocytes (Jo et al., 2014; Park et al., 2009; Yun et al., 2011). In our study, the increase in Cav-2 expression was seen mainly in endothelial cells but barely observed in other glial cells in the aged mouse brain. It would be interesting to compare and analyze the expression patterns and functional differences between Cav-1 and Cav-2 according to the types of cells in the brain, under various neurodegenerative conditions, such as ROS-mediated oxidative stress, inflammation, and aging.

We found that mRNA and protein levels of PECAM1 (CD31) and VE-cadherin (cadherin-5, CD144), as well as Cav-2, were increased in the aged group. PECAM1 is a 130 kDa glycoprotein expressed on endothelial cells, platelets, and leukocytes (Woodfin et al., 2007). In endothelial cells, PECAM1 is localized at intercellular junctions, playing an important role in the adhesion of endothelial cells and transendothelial migration of leukocytes (Muller et al., 1993). VE-cadherin is a type I transmembrane protein that is expressed in endothelial cells and participates in barrier function and transendothelial migration (Allingham et al., 2007; Duong and Vestweber, 2020). Consistent with these previous reports, our results also show an increase in PECAM1 and VE-cadherin expression in aged wild-type mice, and this upregulation is thought to contribute to the increased infiltration of leukocytes in the brain through aiding the adhesion and transendothelial migration. Previous studies have revealed that Cav-2 interacts and colocalizes with connexin 43 in rat epidermal keratinocytes, suggesting that Cav-2 regulates gap junctional intercellular communication (Langlois et al., 2008) and that Cav-2 may work with these cell adhesion molecules. Since increased expression of VE-cadherin and PECAM1 in brain tissues was not observed in aged Cav-2 KO mice, this phenomenon appears to be Cav-2-dependent. However, when the expression level of PECAM1 and VE-cadherin was analyzed after overexpression or knockdown of Cav-2 in HUVECs, no significant change was observed (data not shown). This suggests that rather than Cav-2 directly regulating PECAM1 and VE-cadherin expression, the expression of these proteins was likely indirectly increased by Cav-2 via inflammatory cells and increased chemokine production. Our results demonstrate that the increased neuroinflammatory profiles of aged wild-type mice are dependent on increased Cav-2 expression in brain endothelial cells, at least in part, as we could hardly observe these inflammatory profiles in the brain of aged Cav-2 KO mice (Fig. 7). To the best of our knowledge, this is the first report to address the effect of Cav-2 upregulation in endothelial cells of aged mouse brain on cell adhesion, transendothelial migration, and neuroinflammation. These findings support the notion that Cav-2 may play a key role in leukocyte/neutrophil adhesion and infiltration, leading to an increase in chemokine expression and neuroinflammation in the aging brain.

Note: Supplementary information is available on the Molecules and Cells website (www.molcells.org).

ACKNOWLEDGMENTS

This work was supported by a National Research Foundation of Korea (NRF) grant funded by NRF-2019R1A2B5B01070674 and 2020R1A5A2019210 (Y.-H.C.) and by the RP-Grant 2019 of Ewha Womans University (H.P.) and NRF-2021R1C1C1008860 (J.A.S.).

AUTHOR CONTRIBUTIONS

Y.-H.C., H.P., and J.A.S. conceived and designed the research. H.P. and J.A.S. performed most of biological experiments. J.L. performed data mining and bioinformatics of gene/protein expression. S.L. provided methodological and scientific assistance. J.-H.A. and J.L.K. contributed mouse models/samples. Y.-H.C., H.P., J.A.S., and J.L. wrote the manuscript. Y.-H.C. orchestrated data integration and prepared the manuscript.

CONFLICT OF INTEREST

The authors have no potential conflicts of interest to disclose.

ORCID

Hyunju Park	https://orcid.org/0000-0001-7742-9540
Jung A Shin	https://orcid.org/0000-0002-4014-4282
Jiwoo Lim	https://orcid.org/0000-0002-8071-1384
Seulgi Lee	https://orcid.org/0000-0001-7184-7215
Jung-Hyuck Ahn	https://orcid.org/0000-0001-9589-3881
Jihee Lee Kang	https://orcid.org/0000-0003-0998-3712
Youn-Hee Choi	https://orcid.org/0000-0002-7971-9493

REFERENCES

Allingham, M.J., van Buul, J.D., and Burridge, K. (2007). ICAM-1-mediated, Src- and Pyk2-dependent vascular endothelial cadherin tyrosine phosphorylation is required for leukocyte transendothelial migration. J. Immunol. *179*, 4053-4064.

Chakrabarti, S., Munshi, S., Banerjee, K., Thakurta, I.G., Sinha, M., and Bagh, M.B. (2011). Mitochondrial dysfunction during brain aging: role of oxidative stress and modulation by antioxidant supplementation. Aging Dis. *2*, 242-256.

de Almeida, C.J., Witkiewicz, A.K., Jasmin, J.F., Tanowitz, H.B., Sotgia, F., Frank, P.G., and Lisanti, M.P. (2011). Caveolin-2-deficient mice show increased sensitivity to endotoxemia. Cell Cycle *10*, 2151-2161.

Drab, M., Verkade, P., Elger, M., Kasper, M., Lohn, M., Lauterbach, B.,

Menne, J., Lindschau, C., Mende, F., Luft, F.C., et al. (2001). Loss of caveolae, vascular dysfunction, and pulmonary defects in caveolin-1 gene-disrupted mice. Science *293*, 2449-2452.

Duong, C.N. and Vestweber, D. (2020). Mechanisms ensuring endothelial junction integrity beyond VE-cadherin. Front. Physiol. *11*, 519.

Duxbury, M.S., Ito, H., Ashley, S.W., and Whang, E.E. (2004). CEACAM6 cross-linking induces caveolin-1-dependent, Src-mediated focal adhesion kinase phosphorylation in BxPC3 pancreatic adenocarcinoma cells. J. Biol. Chem. *279*, 23176-23182.

Finger, C.E., Moreno-Gonzalez, I., Gutierrez, A., Moruno-Manchon, J.F., and McCullough, L.D. (2022). Age-related immune alterations and cerebrovascular inflammation. Mol. Psychiatry *27*, 803-818.

Flanary, B.E., Sammons, N.W., Nguyen, C., Walker, D., and Streit, W.J. (2007). Evidence that aging and amyloid promote microglial cell senescence. Rejuvenation Res. *10*, 61-74.

Guo, J., Liao, M., Hu, X., and Wang, J. (2021). Tumour-derived Reg3A educates dendritic cells to promote pancreatic cancer progression. Mol. Cells *44*, 647-657.

Han, K.H., Lim, J.M., Kim, W.Y., Kim, H., Madsen, K.M., and Kim, J. (2005). Expression of endothelial nitric oxide synthase in developing rat kidney. Am. J. Physiol. Renal Physiol. *288*, F694-F702.

Han, K.H., Woo, S.K., Kim, W.Y., Park, S.H., Cha, J.H., Kim, J., and Kwon, H.M. (2004). Maturation of TonEBP expression in developing rat kidney. Am. J. Physiol. Renal Physiol. *287*, F878-F885.

Hefendehl, J.K., Neher, J.J., Suhs, R.B., Kohsaka, S., Skodras, A., and Jucker, M. (2014). Homeostatic and injury-induced microglia behavior in the aging brain. Aging Cell *13*, 60-69.

Hickman, S., Izzy, S., Sen, P., Morsett, L., and El Khoury, J. (2018). Microglia in neurodegeneration. Nat. Neurosci. *21*, 1359-1369.

Jeon, B.K., Kwon, K., Kang, J.L., and Choi, Y.H. (2015). Csk-induced phosphorylation of Src at tyrosine 530 is essential for H2O2-mediated suppression of ERK1/2 in human umbilical vein endothelial cells. Sci. Rep. *5*, 12725.

Jo, A., Park, H., Lee, S.H., Ahn, S.H., Kim, H.J., Park, E.M., and Choi, Y.H. (2014). SHP-2 binds to caveolin-1 and regulates Src activity via competitive inhibition of CSK in response to H2O2 in astrocytes. PLoS One *9*, e91582.

Kim, H.J., Song, D.E., Lim, S.Y., Lee, S.H., Kang, J.L., Lee, S.J., Benveniste, E.N., and Choi, Y.H. (2011). Loss of the promyelocytic leukemia protein in gastric cancer: implications for IP-10 expression and tumor-infiltrating lymphocytes. PLoS One *6*, e26264.

Krajewska, W.M. and Maslowska, I. (2004). Caveolins: structure and function in signal transduction. Cell. Mol. Biol. Lett. *9*, 195-220.

Langlois, S., Cowan, K.N., Shao, Q., Cowan, B.J., and Laird, D.W. (2008). Caveolin-1 and -2 interact with connexin43 and regulate gap junctional intercellular communication in keratinocytes. Mol. Biol. Cell *19*, 912-928.

Le Lay, S., Hajduch, E., Lindsay, M.R., Le Liepvre, X., Thiele, C., Ferre, P., Parton, R.G., Kurzchalia, T., Simons, K., and Dugail, I. (2006). Cholesterol-induced caveolin targeting to lipid droplets in adipocytes: a role for caveolar endocytosis. Traffic *7*, 549-561.

Lu, T., Aron, L., Zullo, J., Pan, Y., Kim, H., Chen, Y., Yang, T.H., Kim, H.M., Drake, D., Liu, X.S., et al. (2014). REST and stress resistance in ageing and Alzheimer's disease. Nature *507*, 448-454.

Lu, T., Pan, Y., Kao, S.Y., Li, C., Kohane, I., Chan, J., and Yankner, B.A. (2004). Gene regulation and DNA damage in the ageing human brain. Nature *429*, 883-891.

McHugh, D. and Gil, J. (2018). Senescence and aging: causes, consequences, and therapeutic avenues. J. Cell Biol. *217*, 65-77.

Melov, S. (2000). Mitochondrial oxidative stress. Physiologic consequences and potential for a role in aging. Ann. N. Y. Acad. Sci. *908*, 219-225.

Muller, W.A., Weigl, S.A., Deng, X., and Phillips, D.M. (1993). PECAM-1 is required for transendothelial migration of leukocytes. J. Exp. Med. *178*, 449-460.

Navarro, A., Anand-Apte, B., and Parat, M.O. (2004). A role for caveolae in cell migration. FASEB J. *18*, 1801-1811.

Niccoli, T. and Partridge, L. (2012). Ageing as a risk factor for disease. Curr. Biol. *22*, R741-R752.

Oberdoerffer, P., Michan, S., McVay, M., Mostoslavsky, R., Vann, J., Park, S.K., Hartlerode, A., Stegmuller, J., Hafner, A., Loerch, P., et al. (2008). SIRT1 redistribution on chromatin promotes genomic stability but alters gene expression during aging. Cell *135*, 907-918.

Parat, M.O. (2009). The biology of caveolae: achievements and perspectives. Int. Rev. Cell Mol. Biol. *273*, 117-162.

Park, H., Ahn, S.H., Jung, Y., Yoon, J.C., and Choi, Y.H. (2017). Leptin suppresses glutamate-induced apoptosis through regulation of ERK1/2 signaling pathways in rat primary astrocytes. Cell. Physiol. Biochem. *44*, 2117-2128.

Park, S.J., Kim, H.Y., Kim, H., Park, S.M., Joe, E.H., Jou, I., and Choi, Y.H. (2009). Oxidative stress induces lipid-raft-mediated activation of Src homology 2 domain-containing protein-tyrosine phosphatase 2 in astrocytes. Free Radic. Biol. Med. *46*, 1694-1702.

Park, W.Y., Park, J.S., Cho, K.A., Kim, D.I., Ko, Y.G., Seo, J.S., and Park, S.C. (2000). Up-regulation of caveolin attenuates epidermal growth factor signaling in senescent cells. J. Biol. Chem. *275*, 20847-20852.

Parolini, I., Sargiacomo, M., Galbiati, F., Rizzo, G., Grignani, F., Engelman, J.A., Okamoto, T., Ikezu, T., Scherer, P.E., Mora, R., et al. (1999). Expression of caveolin-1 is required for the transport of caveolin-2 to the plasma membrane. Retention of caveolin-2 at the level of the golgi complex. J. Biol. Chem. *274*, 25718-25725.

Parton, R.G. and Simons, K. (2007). The multiple faces of caveolae. Nat. Rev. Mol. Cell Biol. *8*, 185-194.

Razani, B., Engelman, J.A., Wang, X.B., Schubert, W., Zhang, X.L., Marks, C.B., Macaluso, F., Russell, R.G., Li, M., Pestell, R.G., et al. (2001). Caveolin-1 null mice are viable but show evidence of hyperproliferative and vascular abnormalities. J. Biol. Chem. *276*, 38121-38138.

Razani, B., Wang, X.B., Engelman, J.A., Battista, M., Lagaud, G., Zhang, X.L., Kneitz, B., Hou, H., Jr., Christ, G.J., Edelmann, W., et al. (2002). Caveolin-2-deficient mice show evidence of severe pulmonary dysfunction without disruption of caveolae. Mol. Cell. Biol. *22*, 2329-2344.

Rea, I.M., Gibson, D.S., McGilligan, V., McNerlan, S.E., Alexander, H.D., and Ross, O.A. (2018). Age and age-related diseases: role of inflammation triggers and cytokines. Front. Immunol. *9*, 586.

Reiter, E., Jiang, Q., and Christen, S. (2007). Anti-inflammatory properties of alpha- and gamma-tocopherol. Mol. Aspects Med. *28*, 668-691.

Scherer, P.E., Lewis, R.Y., Volonte, D., Engelman, J.A., Galbiati, F., Couet, J., Kohtz, D.S., van Donselaar, E., Peters, P., and Lisanti, M.P. (1997). Cell-type and tissue-specific expression of caveolin-2. Caveolins 1 and 2 co-localize and form a stable hetero-oligomeric complex in vivo. J. Biol. Chem. *272*, 29337-29346.

Sevenich, L. (2018). Brain-resident microglia and blood-borne macrophages orchestrate central nervous system inflammation in neurodegenerative disorders and brain cancer. Front. Immunol. *9*, 697.

Shmuel, M., Nodel-Berner, E., Hyman, T., Rouvinski, A., and Altschuler, Y. (2007). Caveolin 2 regulates endocytosis and trafficking of the M1 muscarinic receptor in MDCK epithelial cells. Mol. Biol. Cell *18*, 1570-1585.

Snowdon, V., Hay, R.W., and Demetrick, D.J. (2007). Mitochondrial DNA analysis of acellular laboratory samples. Am. J. Clin. Pathol. *128*, 92-99.

Sowa, G. (2011). Novel insights into the role of caveolin-2 in cell- and tissue-specific signaling and function. Biochem. Res. Int. *2011*, 809259.

Volonte, D. and Galbiati, F. (2020). Caveolin-1, a master regulator of cellular senescence. Cancer Metastasis Rev. *39*, 397-414.

Volonte, D., Zhang, K., Lisanti, M.P., and Galbiati, F. (2002). Expression of caveolin-1 induces premature cellular senescence in primary cultures of murine fibroblasts. Mol. Biol. Cell *13*, 2502-2517.

Wei, Y., Yang, X., Liu, Q., Wilkins, J.A., and Chapman, H.A. (1999). A role for caveolin and the urokinase receptor in integrin-mediated adhesion and signaling. J. Cell Biol. *144*, 1285-1294.

Wheaton, K., Sampsel, K., Boisvert, F.M., Davy, A., Robbins, S., and Riabowol, K. (2001). Loss of functional caveolae during senescence of human fibroblasts. J. Cell. Physiol. *187*, 226-235.

Williams, T.M. and Lisanti, M.P. (2004). The caveolin proteins. Genome Biol. *5*, 214.

Williams, T.M. and Lisanti, M.P. (2005). Caveolin-1 in oncogenic transformation, cancer, and metastasis. Am. J. Physiol. Cell Physiol. *288*, C494-C506.

Woodfin, A., Voisin, M.B., and Nourshargh, S. (2007). PECAM-1: a multi-functional molecule in inflammation and vascular biology. Arterioscler. Thromb. Vasc. Biol. *27*, 2514-2523.

Xie, L., Frank, P.G., Lisanti, M.P., and Sowa, G. (2010). Endothelial cells isolated from caveolin-2 knockout mice display higher proliferation rate and cell cycle progression relative to their wild-type counterparts. Am. J. Physiol. Cell Physiol. *298*, C693-C701.

Xu, S., Zhou, X., Yuan, D., Xu, Y., and He, P. (2013). Caveolin-1 scaffolding domain promotes leukocyte adhesion by reduced basal endothelial nitric oxide-mediated ICAM-1 phosphorylation in rat mesenteric venules. Am. J. Physiol. Heart Circ. Physiol. *305*, H1484-H1493.

Yun, J.H., Park, S.J., Jo, A., Kang, J.L., Jou, I., Park, J.S., and Choi, Y.H. (2011). Caveolin-1 is involved in reactive oxygen species-induced SHP-2 activation in astrocytes. Exp. Mol. Med. *43*, 660-668.

Zhan, Y., Li, Y., and Li, Z. (2017). Preparation of biocompatible near-infrared fluorescent nanoparticles for cellular imaging. J. Nanosci. Nanotechnol. *17*, 1530-1533.

Zia, A., Pourbagher-Shahri, A.M., Farkhondeh, T., and Samarghandian, S. (2021). Molecular and cellular pathways contributing to brain aging. Behav. Brain Funct. *17*, 6.

Zou, H., Stoppani, E., Volonte, D., and Galbiati, F. (2011). Caveolin-1, cellular senescence and age-related diseases. Mech. Ageing Dev. *132*, 533-542.